5-3-2024

3D Printing Applications for NASA Human Exploration Rover Challenge (HERC) Task Tool Use

Grace Marie Pennington
University of Alabama in Huntsville

3D Printing Applications for NASA Human Exploration Rover Challenge (HERC) Task Tool Use

by

Grace Marie Pennington

An Honors Capstone

submitted in partial fulfillment of the requirements

for the Honors Diploma

to

The Honors College

of

The University of Alabama in Huntsville

May 3, 2024

Honors Capstone Project Director: Mr. David Fikes

Grace Pennington 5/3/24

Student Date

David Fikes 5/3/24

Project Director Date

5/3/24

Department Chair Date

Sean Lane Digitally signed by Sean Lane
Date: 2024.05.05 09:37:34
-05'00'

Honors College Dean Date

HONORS COLLEGE
THE UNIVERSITY OF ALABAMA IN HUNTSVILLE

Honors College

Frank Franz Hall

+1 (256) 824-6450 (voice)

+1 (256) 824-7339 (fax)

honors@uah.edu

Honors Thesis Copyright Permission

This form must be signed by the student and submitted with the final manuscript.

In presenting this thesis in partial fulfillment of the requirements for Honors Diploma or Certificate from The University of Alabama in Huntsville, I agree that the Library of this University shall make it freely available for inspection. I further agree that permission for extensive copying for scholarly purposes may be granted by my advisor or, in his/her absence, by the Chair of the Department, Director of the Program, or the Dean of the Honors College. It is also understood that due recognition shall be given to me and to The University of Alabama in Huntsville in any scholarly use which may be made of any material in this thesis.

Grace Pennington
____
Student Name (printed)

Grace Pennington
____
Student Signature

5/3/24
____
Date

Table of Contents

Abstract

Additive manufacturing, specifically 3D printing, has become increasingly common for engineering applications. The cost, weight, and material saved with each piece make 3D printing an excellent tool for low-cost low-risk engineering. However, some 3D printed components have reduced strength for certain high-loading applications. The University of Alabama in Huntsville (UAH) team for the NASA Human Exploration Rover Challenge (HERC) incorporated a number of 3D printed components into the challenge's Task Tool design. These components include a snake light mount, a manual release hinge, and a custom grabber. This project analyzed the design and performance of the Task Tool with functional testing and measurement. Identified weaknesses were addressed and the HERC team won first place in the college division with the robust and versatile Task Tool.

Chapter 1: A Brief History of HERC

NASA's Human Exploration Rover Challenge began with the Great Moonbuggy Race. In 1994, NASA hosted the first Moonbuggy, or rover, race at the original lunar roving vehicle (LRV) testing grounds on Redstone Arsenal, Huntsville, AL. The race course was designed to simulate challenges that a real lunar vehicle might encounter on the Moon. A team from the University of Alabama in Huntsville (UAH) participated in that first race, one of eight college teams [1]. The original race included no tasks, instead challenging students to add rover equipment simulators to their rovers.

Figure 1: UAH Moonbuggy from 1994 [2]

In 1996, the competition moved to the U.S. Space and Rocket Center and opened applications to high school teams as well. With minor changes to the rules for rover construction and performance every year, the Great Moonbuggy Race continued in this form through 2013. In 2014, the race was renamed to the Human Exploration Rover Challenge (HERC) and the race became one of the seven Artemis Student Challenges [4]. These challenges are intended to engage the next generation in STEM fields and foster excitement ahead of NASA's Artemis missions. The Artemis missions plan to land


Figure 2: Original LRV Race Course [3]

the first woman and first person of color on the Moon, as well as establish more permanent footholds in space via a lunar space station during later missions.

The first tasks on the HERC race course would not appear until 2018. In 2018, there were 14 obstacles and 5 tasks on the half-mile course for teams to face. A time limit of 6 minutes challenged students to finish not just fastest but quickly enough to qualify for awards. These tasks "challenged teams to collect and return samples, take photographs and plant a flag" [6]. Teams had to create a tool to help accomplish some of these tasks. As early as 2019, NASA was challenging students to use as much 3D printing as possible [7].

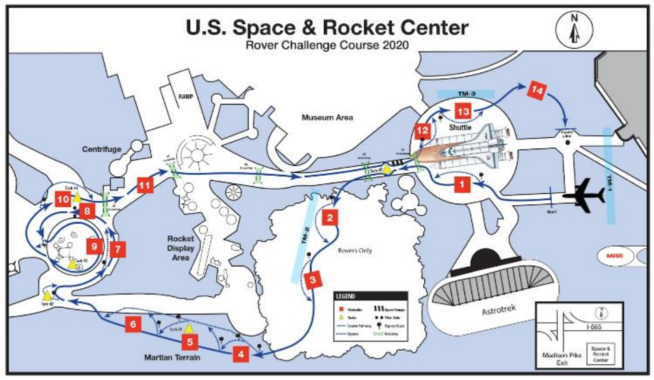

Figure 3: 2020 HERC Race Course [5]

UAH has won first place awards at the 1996, 2012, 2018, 2023 and now 2024 HERC races [8].

Chapter 2: Basics of 3D Printing

Foundation of 3D Printing

The origins of 3D printing, or additive manufacturing, can be traced back to François Willème, a Parisian artist. He developed a method of "photosculpture" where he took 24 photos of a subject in the center of a circular area at 15° intervals (360° in total). From the profiles captured in these pictures, Willème would trace them at the desired scale with a wood-cutter attached to a pantograph. This is regarded as one of the earliest methods of creating a 3D model based on captured data and then producing a physical model based on it. Willème patented photosculpture on August 9, 1864 in U.S. patent 43,822 [9].

Austrian Joseph Blanther, a resident of Chicago, IL, invented a method of forming 3D topographical maps by adding wax. He would take multiple flat sheets of wax and cut out a profile for each altitude interval desired. Then Blanther would stack the cut out profiles to create a 3D topographic map, and could even stack the remains of the layers to create a negative impression map. Since it was made of wax, the rough edges of the map could be smoothed down as needed. This method of additive printing was patented May 3, 1892 [9].

Matsubara of Mitsubishi Motors helped lay the foundation for 3D printing in the following decade. His 1972 proposal for creating a mold started by coating particles of a refractory material in a photopolymer resin and laying the particles out in a thin layer. The layer would be heated to create a "coherent sheet". Then a light would be projected onto the layer to harden the desired slice of a part, and the unhardened remains of the layer would be dissolved away. Repeating this process would form the final mold [10].

Types of 3D Printing

In his 1980s patent, Dr. Hideo Kodama used a photo-hardening polymer and controlled UV exposure to build up materials in layers similarly to Matsubara of Mitsubishi Motors [10, 11]. Largely based on the work of Dr. Kodama, Chuck Hall patented his concept of stereolithography (SLA) in 1984. His patent described a process for taking a CAD model and printing it in successive thin layers by containing a material that can be hardened, e.g. a UV curable material, and hardening it layer by layer [12]. These methods of 3D printing are the first known methods to print the deliverable directly instead of indirectly. Chuck Hall was also one of the first to create a commercial 3D printing apparatus, co-founding 3D Systems, Inc. which made the SLA-1 in 1987 [11].

Shortly after Chuck Hall's work in the 1980s, student Carl Deckard developed Selective Laser Sintering (SLS). He proposed a machine that could use a laser to sinter a powdered material, layer by layer, to form a final piece via additive manufacturing. Sintering is different from melting, as sintering specifically describes heating a material below the melting point to form one continuous object [13]. One of the most significant differences between SLS and SLA is that SLS can be used with any meltable powdered material. While SLA is typically used with resins or other UV hardening materials, SLS can be used with nylons, plastics, metals, and more [14]. SLS can be categorized as a type of laser additive manufacturing, which describes a family of similar powder melting laser manufacturing techniques [15].

Fused deposition modeling (FDM) was developed in 1989 by Scott and Lisa Crump [11]. In FDM, a filament material, typically a polymer, is heated and then extruded through a nozzle onto the print bed. The nozzle is controlled by G-code similarly to CNC machining. The G-code which is typically generated from a CAD file controls the direction, speed, and extrusion of the nozzle on the print bed. The filament is extruded layer by layer. Many commercially available printers today are FDM printers. There are many types of FDM filaments, a few of which are listed below in Table 2.1.

Table 2.1: FDM Filaments for 3D Printing [16]

Filament	**Rigid**	**Brittle**	**Durable**	**Prone to Warping**	**Melting Point [°C]**	**UV-Sensitive**	**Adhesion Issues**
PLA	Yes	Yes	No	No	180-220	Yes	Minimal
PETG	Yes	No	Yes	No	220-260	No	Yes

ABS	Yes	No	Yes	Yes	220-250	Yes	Yes
TPU	No	No	Yes	No	~230	No	No
Nylon	Yes	No	Yes	Yes	230-260	Yes	No
Carbon Fiber (additive)	Yes	Yes	Yes	No	--	No	Yes

Process of FDM 3D Printing

3D printing begins with a CAD file. The UAH HERC team uses the CAD program Autodesk Inventor since it is free to students, hosts collaborative work, and is powerful enough to meet the needs of the project. Next the CAD model must be exported as an .stl file. .stl files were developed by 3D Systems and Albert Consulting Group for Chuck Hall's stereolithography. The file type tessellates the outer surface of a 3D model and stores the vertex coordinates and unit normal vector of each triangle, or facet. There are other file types one can use for 3D printing, but the .stl is still the most common [20]. The UAH HERC team uses .stl files with its printers.

To print the model, the .stl file is next put into a slicer program. Many 3D printers have their own proprietary slicers, but they all serve the same general purpose. A slicer takes the .stl file and analyzes it in horizontal layers, calculating where to apply material, print speed, support structures, and more for each layer of the print. The slicer writes this print data in G-code, the same sort of code which controls a CNC mill [17].

Before printing, the print bed of the printer must be clean and level. For proper print bed adhesion of the first layer of the print, there must be no dust or skin oils on the print bed. Wiping the print bed with isopropyl alcohol is sufficient to clean. Many printers have self-leveling features to ensure that the print can adhere to the surface of the print bed and prevent collisions with the print bed. The UAH HERC team used two 3D printers to print the Task Tool components: the Prusa I3 MK3S+ and Bambu Lab P1P. Select properties of both printers are shown in Table 2.2.

Table 2.2: Properties of Available Commercial 3D Printers [18, 19]

	Prusa	**Bambu Lab P1P**
Build Volume [mm^3]	250 × 210 × 210	256 × 256 × 256
Layer Height [mm]	0.05 - 0.35	[Nozzle dependent]
Maximum Nozzle Temperature [°C]	300	300
Maximum Heatbed Temperature [°C]	120	100
Maximum Travel Speed [mm/s]	200+	500

Chapter 3: UAH Task Tool Development

Previous UAH Task Tools

Figure 4: 2020 Spectrometer Prototype [20]

The 2019-2020 UAH HERC team had designed a primarily 3D-printed Task Tool. The tasks were markedly different from the 2023-2024 tasks. The 2019-2020 Task Tool had tools to take liquid samples, solid samples (see Fig. 5), and photograph using different color filters (see Fig. 4). The team used light materials such as carbon fiber body tubing and PLA 3D printing filament to minimize the overall weight of their Task Tool while still meeting NASA's 3D printed component challenge requirements [7].

Figure 5: 2020 Core Sampler Prototype [20]

The 2020-2021 UAH HERC team inherited much of the work from the 2019-2020 team, since COVID-19 shutdowns prevented an in-person competition from happening in April 2020. Even into 2021-2022, there is not significant remaining documentation indicating that major revisions were occurring. In 2022-2023, the UAH HERC team did significantly change their Task Tool, and it involved 3D printed components. The carbon fiber body of earlier Task Tools was preserved, but a metal hook to uncover hidden liquid sampling sites was added. Custom motor housings, custom liquid sample containers, and even a custom bucket for taking liquid samples only accessible through a high reach spot were all added during this year [21]. Several of these components are visible in Fig. 6. 3D printed components for non-load bearing functions helped keep a heavy Task Tool lighter and met unique needs that would have been difficult to find in COTS parts.

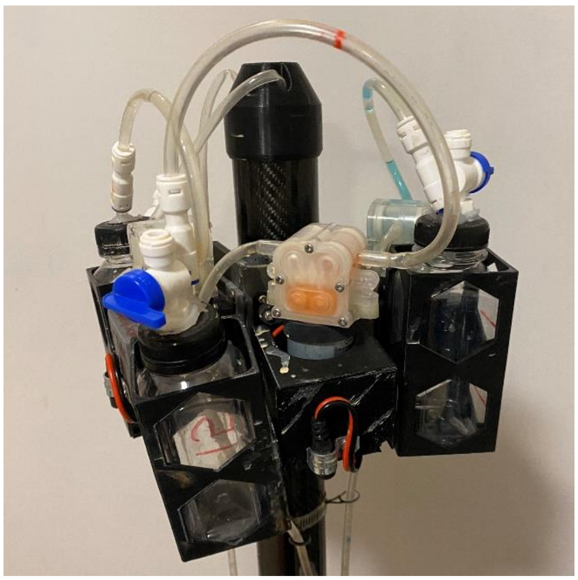

Figure 6: 2023 Task Tool Detail

HERC 2024 Tasks

Task 1: Find ARV-30 simulated a 2-person crew using a light to examine a robotic rover in a Permanently Shadowed Region (PSR) on the Moon. The pilots would be required to activate a photosensor kept in complete darkness on the course with the Task Tool to complete the task and earn full points. No further details were provided regarding how the photosensor would be kept in darkness or how sensitive it would be.

Task 2: Regolith Removal simulated the 2-person crew cleaning the solar panels of the robotic rover. A solar panel 3 ft above the ground would be inclined at a 45° angle and the regolith would need to be removed by the Task Tool without causing damage to or moving the solar panels. When sufficiently cleared, an indicator light would be activated. The exact solar panel size and materials used in this task were not specified.

Task 3: Moon Maintenance did not require the Task Tool. One pilot would dismount the rover and use NASA-provided gloves and a hand tool to simulate an astronaut in an EVA suit removing a cover plate on the robotic rover. This task was one that challenged pilot skill, not one that challenged Task Tool designs.

Task 4: Power It Up simulated the pilot recharging the robotic rover's batteries. The Task Tool would be used to attach two connected battery cable clamps to simulated battery posts. The clamps would take a maximum of 15 lbs of force to open, and the handles would not open wider than 3 in. The battery posts would be 4 in long, with one post perpendicular to and 3 ft above the ground and one post pointing towards the rider at around 46 in above the ground.

Task 5: Rover Redundancy simulates the pilot retrieving test samples from the robotic rover and storing them on the pilot's rover. Four sample containers with a diameter of around 2 *in* and a length of 4-6 *in* would be removed from the task site and stored on the rover. The task site would store the samples vertically in various configurations with at least a full diameter grip available. Samples must be retrieved from the test site by the Task Tool but could be moved between the Task Tool and the on-rover storage by hand.

Design & Testing Overview

The 2023-2024 Task Tool is composed of multiple tools attached to a 1 *in.* square aluminum tubing frame. Attached to the body are a gripper, 2 brake cable mounts, handle, brake handle, hinge, folding latch, snake light mount, and broom attachment point. The snake light meets the requirements of Task 1, capable of shining light in multiple directions to activate the photosensor however it is mounted. The broom is designed to complete Task 2 by clearing the regolith from the solar panel without causing scratches or damage. The gripper will be able to complete both Tasks 4 and 5, having the strength to open the battery clamps and the dexterity to retrieve 4 samples from their previous mounts. The hinging design of the Task Tool allows it to extend if the solar panel is too large to reach while still folding small enough to fit in the 5 *ft* x 5 *ft* x 5 *ft* cube that the full rover must fit into.

The aluminum frame of the Task Tool is designed to provide strength while still being relatively lightweight. Its square shape enables easier attachment of components. The braking components in the gripper, bearings in the gripper, screws throughout the Task Tool, broom, and snake light are all commercial off-the-shelf (COTS) components. All other components are 3D printed with 1.75 *mm* PETG filament. PETG filament was chosen for its strength and durability, ideal qualities for Task Tool purposes. 3D printed parts are also notably lighter than comparative metal parts, reducing weight. Reducing weight and increasing versatility are the main goals when designing the Task Tool, and 3D printed components play a strong role in that endeavor.

3D printed components are notoriously difficult to analyze accurately. They are effectively non-uniform composites, because 3D printing slicers can generate non-linear printing paths. Combined with the fact that 3D printed parts are weakest among lamination lines, accurately modeling stresses in a 3D printed part is highly complex. The UAH team decided to emphasize “functional testing” in development of 3D printed components. Functional testing describes the process of testing a component in the way it will be used (e.g. opening and closing a hinge under appropriate loads). The risk of expenses or time-consumption stands, but 3D printing is optimized to minimize them. PETG filament is relatively economical and the small scale of the components being used on the Task Tool helped keep printing times short. In practice, functional testing was more accurate and quicker than in-depth analysis.

Task Tool Gripper

The gripper is composed of a triangular base, 4 moving arms with 608ZZ bearings press-fit into the joints, and 2 jaws formed to grab a target. A brake cable attached to the arms via crimps controls the movement of the gripper. When the brake handle at the end of the Task Tool is closed, the gripper jaws close symmetrically towards a target centered to the gripper.

The gripper is one of the most critical components of the 2023-2024 Task Tool. It is designed to complete two tasks (Task 4 and Task 5), not just one like most other components. The gripper is also the only component with a requirement to exert a specific force. Task 4 requires that the gripper be able to output up to 15 *lb* of

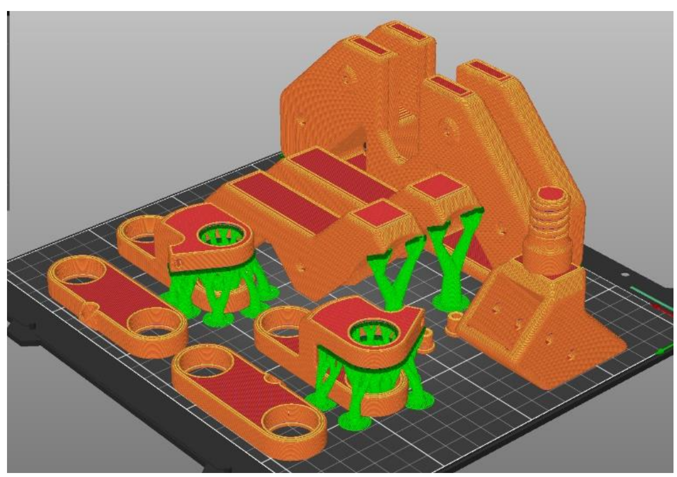

Figure 7: PrusaSlicer Print of Gripper and Broom Components

force. Because of this specific force requirement, the gripper component warranted special testing. To measure the force output of the gripper, Hooke's Law was used.

$$F = kx$$

Hooke's Law relates the displacement *x* of a spring multiplied by the spring constant *k* to the force output *F* of the spring. By measuring how much the gripper could displace a spring with a known spring constant, the force output of the gripper could be measured.

Gripper Testing Materials

Two spring plates were 3D printed from 100% infill PETG. These plates were designed to provide flat surfaces for the grabber to hold the spring by and flat surfaces for the spring to compress between. The walls surrounding the spring have a 0.866 *in* (22 *mm*) diameter to accommodate the changing diameter of the spring as it compresses, and are 0.551 *in* (14 *mm*) tall to prevent the spring from compressing more than its compressed length at maximum load of 1.06 *in* (26.924 *mm*).

The springs used were 3 *in* long, with an outer diameter of 0.66 *in* and ground flat ends. The spring constant was *15.9 lbs./in.* with a maximum total load of 30 *lbs* [22]. Measurements were taken with calipers.

Gripper Testing Procedure

The spring plates were placed at each end of one spring. The initial length of the spring inside of the spring plates was measured. The spring and spring plates were then placed in the jaws of the Task Tool. The spring plates corners were oriented with the Task Tool jaws as follows: the shortest edge of the spring plate was aligned along the tip of the Task Tool arms, and the longest spring plate edge was aligned with the outer edge of the Task Tool arm. The spring was positioned in the spring plate such that the spring touched the walls closest to the tip of the arms. The Task Tool would be held just tight enough to keep the spring in place but not tight enough to compress the spring.

The operator of the Task Tool would then compress the spring as far as they could comfortably with one hand for 10 seconds. At the end of the 10 seconds, the displacement of the spring would be measured with calipers. This process was repeated five times.

Gripper Testing Results and Analysis

The measurements in Table 2.3 were taken with the prototype gripper.

Table 2.3: Prototype Gripper Data	
Test	**Compressed Length [in]**
No Load	3.004
1	2.403
2	2.369
3	2.435
4	2.352
5	2.299

The measurements in Table 2.4 were taken with the final gripper.

Table 2.4: Final Gripper Data	
Test	**Compressed Length [in]**
No Load	3.01
1	1.939
2	1.804
3	1.955
4	1.916
5	1.935

Due to the small sample size, both Chauvenet's criterion and the Student's t-series were applied to the data gathered during these experiments. For the prototype gripper, Table 2.5 shows the results of these calculations. Note that no outliers were identified in the data from Table 2.3.

Table 2.5: Prototype Gripper Data Analysis	
Average	2.3716
Standard Deviation S_x	0.051641069
$\bar{S}_x$	0.023094588
λ	1.65
P_x	0.110098759
$\bar{P}_x$	0.049237662
P_{min}	2.322362338
P_{max}	2.420837662
$P\%$	4.642383157

For the final gripper, Table 2.6 shows the results of these calculations. Note that one outlier, Test 2 in Table 2.4, was identified. This outlier was removed from calculations afterwards.

Table 2.6: Final Gripper Data Analysis	
Average	1.9098
Standard Deviation S_x	0.060751132
$\bar{S}_x$	0.027168732
λ	1.65
Average	1.93625
Standard Deviation S_x	0.01602862
$\bar{S}_x$	0.00801431
P_x	0.034173018
$\bar{P}_x$	0.017086509
P_{min}	1.919163491
P_{max}	1.953336509
P_x	1.764907339

The results of the prototype gripper showed that while it was possible to exert a load of 15 *lbs* on an object, it was not easy or comfortable for a rider to do so. The average force comfortably exerted by the prototype gripper was 10.055 *lbs*. It was decided to make changes to the gripper to change this.

The gripper arms were modified to shorten the arm springs which keep the gripper open. This reduced the negative force exerted by the arm springs, minimizing the force needed to close the gripper. The brake cable material also switched from uncoated steel cable to teflon-coated steel cable. The results of these changes are clearly visible in the data taken from the final gripper.

The average force comfortably exerted by the rider increased to 17.073 *lbs.* This shows that a Task Tool operator should be able to comfortably exert the required 15 *lbs*. of force with one hand. This most accurately simulates how the Task Tool will be used on the course.

There is uncertainty with these readings. If the spring was not perfectly perpendicular to the gripper jaws, or if the gripper jaws were not parallel, that could have added error to the results. The same concept applies to the calipers used to measure spring displacement. Lastly, the force applied during each test is subject to variation as humans do not usually apply the same load exactly every time.

The variance in measurement and force did not significantly impact the precision of the data, as only one outlier across all data was identified by Chauvenet's criterion. Also consider the confidence intervals of the data. With a low 90% confidence, the probable ranges of comfortable force are 9.272-10.838 *lbs*. for the prototype gripper and 16.801-17.344 *lbs.* for the final gripper. These results are considered strong enough to show that the Task Tool is capable of meeting the 15 *lbs*. force requirement.

Task Tool Brake Cable Mount

The brake cable mount holds the brake cable casing along the body of the Task Tool. The mount closest to the gripper has a lip which holds the brake cable casing in place. The first iteration of this brake cable casing broke when the gripper was closed too hard and the force from holding the brake cable casing in place sheared half of the component off. This shear is shown in Fig. 6. By increasing the lip of the brake cable mount, the strength of the mount was sufficient to secure the brake cable casing in place.

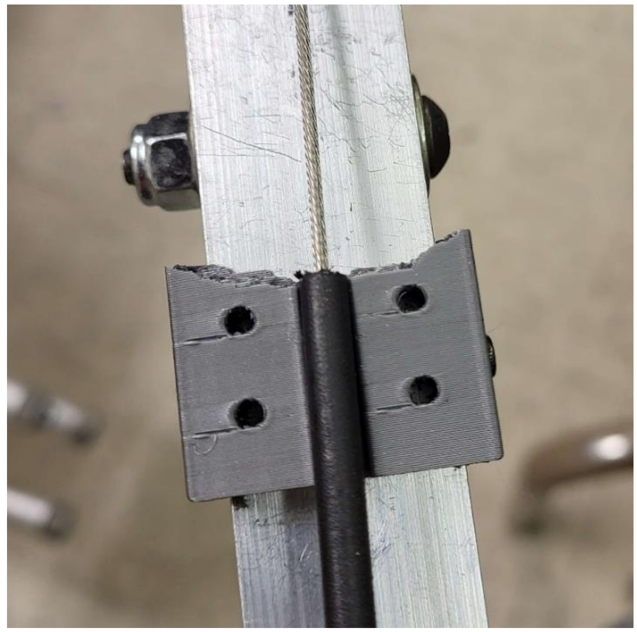

Figure 8: Brake Cable Mount Failure

Task Tool Hinge

The hinge of the Task Tool endures two critical stresses. First, the actual hinging mechanism must be able to bear both the weight of the Task Tool and the force delivered upon opening the Task Tool. Second, the clipping mechanism must be able to hold the Task Tool in the open position. In the first iteration of the hinge, the full piece was 100% infill PETG with the exception of the hinging mechanism's bolt, which was a screw.

The clip started off as fully 3D printed material, but the clipping mechanism broke very quickly. It sheared through the thinnest part of the clip, clearly not capable of meeting the load requirements. On the next iteration of the hinge, the clipping mechanism thickness was increased to the point of difficulty using the hinge but still eventually broke. It was eventually determined that the hinge was too great a point of failure to not use a stronger design. The clipping mechanism was reinforced with a bolt similar to the main hinging mechanism, with springs installed to keep the clip closed.

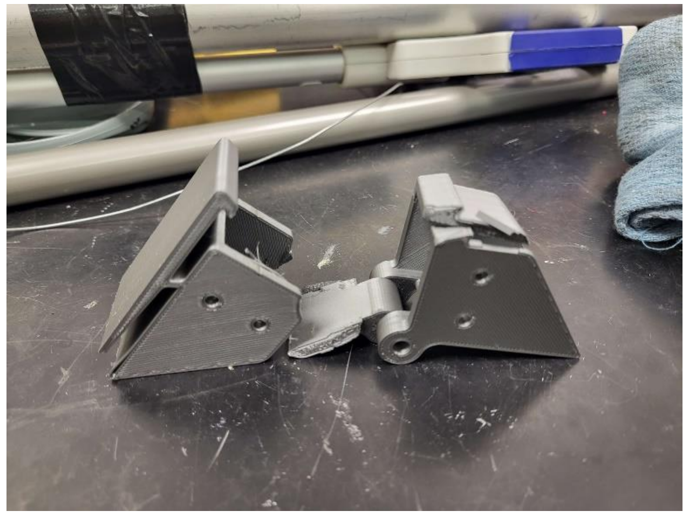

Figure 9: First Hinge Wall Failure

The primary hinging mechanism also experienced failures. Twice, the walls of the hinge fractured. The first fracture was caused by delamination when opening the hinge. One wall of the clip side of the hinge sheared off entirely. This delamination is shown in Fig. 8. The next hinge was printed with tighter tolerances. Still, the next hinge experienced a stress fracture in the same location. Note that this is not regarded as a pure delamination failure because the hinge broke against print layers, indicating that the stress applied to the hinge was simply greater than the strength of the design. This failure is shown in Fig. 9.

Figure 10: Second Hinge Wall Failure

The UAH HERC FEA sub-team performed an analysis of the design of the hinge. The analysis was performed in Patran and is shown in Fig. 10. With the hinge point constrained and a loading approximately equal to the weight of one half of the Task Tool, the analysis verified that the fracture points were high stress areas in the design. To address this issue, the wall thickness of the hinge was increased from 6 *mm* to 8 *mm*. This resolved the issue of fractures at the hinge.

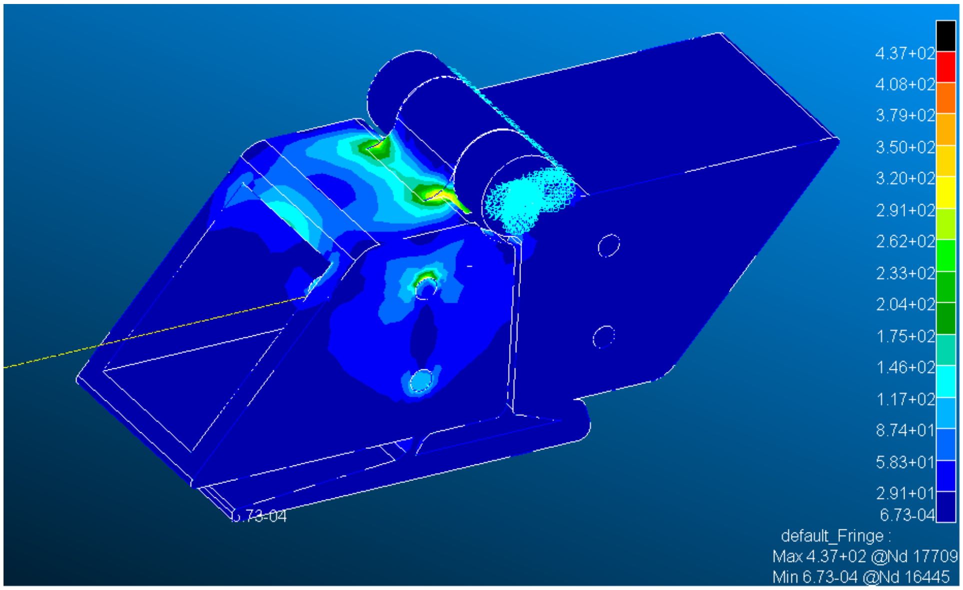

Figure 11: FEA of Hinge

Task Tool Handle

There are two handles on the Task Tool. The first handle is included for stability, to control the grabber more precisely at distance. The second handle is attached to the brake line control that powers the gripper. Both handles have failed once due to delamination during use. To resolve this issue, the thickness of the part walls was increased from 6 *mm* to 8 *mm* and the infill was increased from 30% gyroid infill to 80% cubic infill. Increasing the infill increases the strength of the resulting part. The delamination issue was resolved by this change.

Task Tool Broom and Light Attachment

The broom attachment features a threaded protrusion to which a COTS broom head can be secured by its built-in threads. During rover practice, the pilots would practice changing the orientation of the broom head on the broom attachment for optimized solar panel sweeping. After several weeks of practice, the 3D printed threads became too worn down to hold the broom head in place. To resolve this issue, the broom attachment point was reprinted with thicker threads and the rover pilots implemented techniques to minimize their twisting of the broom head.

The light attachment is a casing for the snake light that can be mounted to the Task Tool. The only notable change to this component is the addition of a velcro pad that helps keep the Task Tool in the closed configuration while stored on the rover. All other changes were cosmetic.

HERC 2024 Course Performance

The Task Tool performed excellently on the HERC course despite encountering obstacles. The tasks on the race course were slightly different than the guidelines provided in the handbook. Most notable were Tasks 2 and 4. The Task 2 solar panel was flat with a surface area of approximately 1-3 ft^2, instead of angled 45°. The battery clamps in Task 4 were not fully 3 *in.* wide and instead significantly smaller. Additionally, it rained before and during both competition days. This meant that all tasks were wet.

On the first day of competition, the Task Tool completed all tasks and finished the course in 5:00 minutes exactly. After completing all Tasks and earning full Task Tool points, the UAH score for day 1 was 182 points out of 200. This put the team in first place for the day. On the second day of competition, the pilots struggled to secure the battery clamps from Task 4 in the gripper. After several seconds of struggle, Task 4 was successfully completed. The final time of run two was 5:33. It is worth noting that while some of this additional time came from Task 4, some of this time came from attempting more obstacles on day 2. After completing all tasks for the second day in a row, the UAH team scored 187 points out of 200 for day 2. This score won the UAH team 1st place in the college division of HERC.

Conclusion

3D printing is an extremely useful material when being used for weight-sensitive, low strength, prototyping development needs. By including more 3D printed components, the UAH HERC Team created and tested all the necessary components of a Task Tool. Repeated testing highlighted areas where design revision was necessary and validated successful designs. The Task Tool performed extremely well during the HERC race and helped secure a victory for UAH. Future teams should consider integrating 3D printed components into their Task Tools, and if done should also perform effective functionality testing and analysis.

Reference List

[1] Frost, Larry D. "UAH Team Wins First Place at NASA's Great Moonbuggy Race (4/2012)." The University of Alabama in Huntsville, April 16, 2012. https://www.uah.edu/eng/engineering-news/352-engnewsarchive/2337-engnews-moonbuggyrace.

[2] NASA. "Great Moonbuggy Race, 1994." NASA. April 22, 2013. https://www.nasa.gov/image-article/great-moonbuggy-race-1994/.

[3] NASA. "6973609." NASA. March 1, 1969. https://images.nasa.gov/details/6973609.

[4] NASA STEM. "Artemis Student Challenges." NASA. https://www.nasa.gov/wp-content/uploads/2021/04/asc_flyer.pdf

[5] Mohon, Lee. "NASA Opens Registration for 2020 Human Exploration Rover Challenge." NASA. October 10, 2019. https://www.nasa.gov/centers-and-facilities/marshall/nasa-opens-registration-for-2020-human-exploration-rover-challenge/

[6] Mohon, Lee. "NASA Announces Winners of Weather-shortened Rover Challenge." NASA. April 15, 2018. https://www.nasa.gov/news-release/nasa-announces-winners-of-weather-shortened-rover-challenge/

[7] Team Falcon and Team Turbochargers. "3D Liquid Tool Report." March 5, 2020. 2021-2022 Moon Buggy. https://docs.google.com/document/d/1D9Hl5-_kTFFgmjifR94K1kylkL3fTztT/edit?usp=sharing&ouid=101949254271626536818&rtpof=true&sd=true

[8] Nelson, Russ. "UAH engineering students top NASA HERC Rover Challenge for second consecutive year." The University of Alabama in Huntsville. April 24, 2024. https://www.uah.edu/news/items/uah-engineering-students-top-nasa-herc-rover-challenge-for-second-consecutive-year

[9] Norman, Jeremy. "François Willème Invents Photosculpture: Early 3D Imaging." History of Information. https://www.historyofinformation.com/detail.php?id=3876

[10] Beaman, Joseph J. "Solid Freeform Fabrication: An Historical Perspective." *2001 International Solid Freeform Fabrication Symposium*: 585-593. http://dx.doi.org/10.26153/tsw/3354.

[11] González, Carlos M. “Infographic: The History of 3D Printing.” ASME. January 30, 2020. https://www.asme.org/topics-resources/content/infographic-the-history-of-3d-printing.

[12] Hull, Charles W. 1984. Apparatus for production of three-dimensional objects by stereolithography. Unites States of America. US4575330A, filed August 8, 1984, and issued March 11, 1986.

[13] Britannica, T. Editors of Encyclopaedia. "sintering." Encyclopedia Britannica, March 22, 2024. https://www.britannica.com/technology/sintering.

[14] “Selective Laser Sintering, From a Texas Idea to a Global Industry.” The University of Texas at Austin Walker Department of Mechanical Engineering. (https://www.me.utexas.edu/news/619-selective-laser-sintering-from-a-texas-idea-to-a-global-industry)

[15] Kh. Moeinfar, F. Khodabakhshi, S.F. Kashani-bozorg, M. Mohammadi, A.P. Gerlich. “A review on metallurgical aspects of laser additive manufacturing (LAM): Stainless steels, nickel superalloys, and titanium alloys.” Journal of Materials Research and Technology, Volume 16, 2022: Pages 1029-1068. ISSN 2238-7854. https://doi.org/10.1016/j.jmrt.2021.12.039.

[16] Team Xometry. “Types of 3D Printer Filaments.” Xometry. September 12, 2022. https://www.xometry.com/resources/3d-printing/types-of-3d-printer-filaments/

[17] All3DP. “What Is an STL File? – The STL Format Simply Explained.” All3DP. May 10, 2023. https://all3dp.com/1/stl-file-format-3d-printing/

[18] “Bambu Lab P1P 3D Printer.” Bambu Lab. https://us.store.bambulab.com/products/p1p

[19] “Original Prusa i3 MK3S+ 3D printer.” Prusa Research. https://www.prusa3d.com/product/original-prusa-i3-mk3s-3d-printer-3/#description

[20] Wexler, Michael, Black, Lauren, Gusewelle, Nathan, Hansen, Noah, Jordan, Quintin, Leyden, Jonathan, McLeod, Alexander, and Methe, Matthew. “Twisted Metal.” January 13, 2020. 2021-2022 Moon Buggy. https://drive.google.com/file/d/17ykISIP7TgVCxefJkxsoSinzBUxvr0Ed/view?usp=sharing

[21] Padilla, Chrys A. and Gray, Colton. “Task Tool ORR.” February 21, 2023. 2022-2023 Moon Buggy. https://docs.google.com/document/d/1Swm8nRukya0hsF9hFkj3EOp41JVtSDctLwioHalF4z0/edit?usp=sharing

[22] “Compression Spring, 3" Long, 0.66" OD, 0.516" ID.” McMaster-Carr. https://www.mcmaster.com/9657K435/